

Designing Tyrosine-Derived Polycarbonate Polymers for Biodegradable Regenerative Type Neural Interface Capable of Neural Recording

Dan Lewitus, R. Jacob Vogelstein, Gehua Zhen, Young-Seok Choi, *Member, IEEE*, Joachim Kohn, Stuart Harshbarger, and Xiaofeng Jia

Abstract—Next-generation neuroprosthetic limbs will require a reliable long-term neural interface to residual nerves in the peripheral nervous system (PNS). To this end, we have developed novel biocompatible materials and a fabrication technique to create high site-count microelectrodes for stimulating and recording from regenerated peripheral nerves. Our electrodes are based on a biodegradable tyrosine-derived polycarbonate polymer system with suitable degradation and erosion properties and a fabrication technique for deployment of the polymer in a porous, degradable, regenerative, multiluminal, multielectrode conduit. The *in vitro* properties of the polymer and the electrode were tuned to retain mechanical strength for over 24 days and to completely degrade and erode within 220 days. The fabrication technique resulted in a multiluminal conduit with at least 10 functioning electrodes maintaining recording site impedance in the single-digit kOhm range. Additionally, *in vivo* results showed that neural signals could be recorded from these devices starting at four weeks postimplantation and that signal strength increased over time. We conclude that our biodegradable regenerative-type neural interface is a good candidate for chronic high fidelity recording electrodes for integration with regenerated peripheral nerves.

Index Terms—Biodegradable, electrode, interface, neuroprosthetics, peripheral nerve, regenerative.

I. INTRODUCTION

Approximately 1.8 million people were estimated to suffer limb loss (excluding finger and toe amputees) in 2010 [1] and more than 185 000 new amputations would be performed in

Manuscript received June 22, 2010; revised September 15, 2010 and November 18, 2010; accepted November 30, 2010. Date of publication December 10, 2010; date of current version April 08, 2011. This work was supported by the Johns Hopkins University Applied Physics Laboratory under the Defense Advanced Research Projects Agency 2009 Revolutionizing Prosthetics program under contract N66001-06-C-8005. The work of X. Jia was also supported in part by the National Institute of Health under Grant RO1 HL071568 and in part by the American Heart Association under Grant 09SDG1110140. The views, opinions, and/or findings contained in this article/presentation are those of the author/presenter and should not be interpreted as representing the official views or policies, either expressed or implied, of the Defense Advanced Research Projects Agency or the Department of Defense. Distribution Statement "A" (Approved for Public Release, Distribution Unlimited).

D. Lewitus and J. Kohn are with the New Jersey Center for Biomaterials, Rutgers, The State University of New Jersey, Piscataway, NJ 08854 USA.

R. G. Vogelstein and S. Harshbarger are with the Johns Hopkins University Applied Physics Laboratory, Laurel, MD 20723 USA.

G. Zhen is with Department of Orthopaedic Surgery, Johns Hopkins University School of Medicine, Baltimore, MD 21205 USA.

Y.-S. Choi was with the Department of Biomedical Engineering, Johns Hopkins University School of Medicine, Baltimore, MD 21205 USA. He is now with the Neural Interface Research Team, Electronics and Telecommunications Research Institute, Daejeon 305700, Korea.

X. Jia is with Department of Biomedical Engineering, Physical Medicine and Rehabilitation, Johns Hopkins University School of Medicine, Baltimore, MD 21205 USA (e-mail: xjia1@jhmi.edu).

Color versions of one or more of the figures in this paper are available online at <http://ieeexplore.ieee.org>.

Digital Object Identifier 10.1109/TNSRE.2010.2098047

the United States [2]. While many of these patients will receive prostheses, the rate of prosthetic rejection remains unsatisfactory at 22%–50%, due in part to lack of functional gain [3]. The two main factors limiting the functionality of prosthetic upper limbs are the lack of a high-bandwidth information channel conveying the user's movement intent and the lack of a high-resolution sensory feedback pathway from the artificial limb. To address these needs, research groups have begun to investigate the feasibility of peripheral nerve interfaces for feedback and control of upper extremity prostheses [3]–[6].

Peripheral nervous system (PNS) interfaces for neural prosthetics provide a reasonable compromise between highly invasive cortical implants [7], [8] and noninvasive control schemes such as those relying on electromyography (EMG) [9], [10]: they achieve higher signal selectivity than EMG but do not provide access to the high-level movement parameters observable in motor cortex. Another option being explored is a procedure known as targeted reinnervation, where residual nerve fibers are meticulously separated and attached to muscle tissue to allow higher fidelity EMG electrode recording [11]. Because the residual peripheral nerves serve limited purpose after upper-limb amputation, a potentially attractive option is to implant multichannel electrodes in the residual components of the peripheral nerves to address the input–output bandwidth limitations described above. The most invasive form of PNS interfaces are regenerative electrodes [12], [13], which require severed nerves to grow and regenerate through an array of electrodes. The benefit of this approach is that it enables direct and stable contact between individual recording sites and growing fascicles, and consequently provides some fidelity advantages over other devices relying on EMG signal. Our group and others have previously demonstrated recording from residual nerves with intraneural devices in human amputees with the use of longitudinal intrafascicular interfaces (LIFEs) [3]–[6] and microelectrode arrays (MEAs) [14], [15].

The most popular design in regenerative electrodes is the sieve electrode of various forms [16], [17]. Recently, long-channel arrays with regenerating nerves growing along individual channels with embedded recording sites have been described. Such channels are primarily based on silicon fabrication techniques (photolithography with material deposition) [18], [19], allowing a larger density of recording sites and a high signal to noise ratio [20]. These devices retain their compartmental structure indefinitely, possibly leading to long-term failure due to compressive forces on the maturing nerve, and the fact that individual fascicles and axons will most likely remain individualized and isolated from nearby tissue and fluid. Moreover, the constant presence of rigid materials has been known to

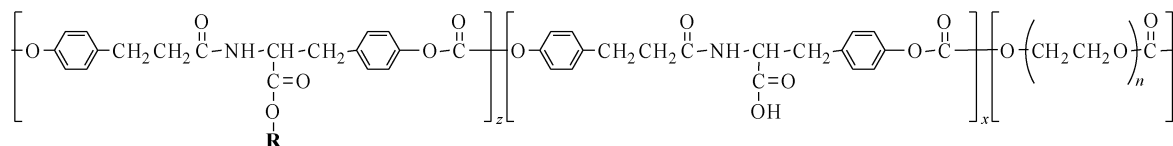


Fig. 1. Structure of tyrosine-derived terpolymers. In our study, the R pendant chain is ethyl.

cause long-term deterioration in maturing regenerating nerves [21], [22]. The use of softer materials reduces the forces acting on the nerves and resultant tissue damage [23], yet does not provide sufficient structural support for the regenerating tissue to retain its conformation [17], [24]. To address some of these issues, Cho *et al.* [25] have lithographically fabricated electrodes and embedded them in a polysaccharide conduit with an outer shell made of polyurethane, a nondegradable, nonporous material.

Our aim is to develop a polymeric system that will allow us to design a biodegradable regenerative-type neural interface (bRTNi) that combines the advantages of many of the approaches described above. Our bRTNi is a multiluminal conduit with embedded electrodes. Taking inspiration from rolled film and multiluminal permeable biodegradable conduit [26]–[29] together with the efficiency of LIFE electrodes [3]–[5], [12], [30]–[33], we have created a regenerative neural interface. The neural interface acts as a multiluminal nerve regeneration conduit with embedded electrodes for recording. Once the polymer degrades, the healthy regenerated nerve should have embedded electrodes remaining within, allowing chronic recording. Our polymer system is based on the most recent generation of the tyrosine-derived polycarbonates. This family of polymers developed over the last 25 years by us and other groups [34]. They have been extensively shown to be biocompatible and biodegradable [35]. Furthermore, acidic environments are not formed upon breakdown into metabolites [36], reducing the chances of causing additional inflammation within injured tissue. The synthesis of copolymers, and more recently terpolymers with the addition of polyethylene glycol (PEG) has shown to modify various polymer physical properties while remaining biocompatible [36]–[38]. We hypothesized that modification of the polymer backbone chemistry would allow us to tune the polymer properties to be compatible with both nerve tissue regeneration rate (1 mm/day) [39], [40] and mechanical properties. The new polymer, developed along with a novel design and fabrication technique, will create a biodegradable scaffold for potential chronic neural recordings. The functionality of the bRTNi design will be evaluated both *in vitro* and *in vivo*.

II. METHODS

A. Polymers and Preparation of Polymer Films

The polymers based on the amino acid L-tyrosine were synthesized via solution polycondensation reactions according to previously published procedures [38], [41]. Polymers were repeatedly precipitated in a suitable nonsolvent and vacuum dried to constant weight. All polymers consist of the basic structure poly (DTR-co-XX%-DT-co-YY%-PEGMW carbonate)s, shown in Fig. 1, with varying amount of all three monomers. To simplify the identification of tyrosine-derived polycarbonates, the following notation in the

form of RXXYY(ZK) will be used to specify different poly (DTR-co-XX%-DT-co-YY%-PEGMW carbonate)s. As an example, poly (DTE-co-25%-DT-co-2%-PEG2K carbonate) will have a notation of E2502 (2K), where E stands for ethyl.

For *in vitro* evaluation of polymer degradation, mass loss, and mechanical properties, porous solvent cast polymer films were prepared by the particulate leaching technique. Polymer powder with the addition of 20% by weight of glucose (G7021, Sigma Aldrich, St. Louis, MO) was dissolved at 10% w/v in tetrahydrofuran (THF, VWR Scientific Products, Radnor, PA) and shaken for 4 h until the polymer was completely dissolved. Solutions were cast into PTFE dishes and left to evaporate overnight under nitrogen in a chemical hood, followed by seven days of drying in vacuum at 40 °C. Films were cut into 5 × 20 mm samples and placed in deionized water for three days at room temperature to allow glucose particulate leaching. Resulting films measured 200 μm thick.

B. Polymer Degradation, Mass Loss In Vitro, Mechanical Testing and Morphology Changes

5 × 40 mm film strips were cut from cast films and placed in 20 mL scintillation vials (Fisher Scientific, Pittsburg, PA) containing prewarmed phosphate buffer saline (PBS, pH 7.4, Sigma Aldrich, St. Louis, MO) and incubated at 37 °C. At predetermined time points, samples ($n = 5$) were visually inspected for integrity, taken out of incubation and used for mechanical testing, then lyophilized for 96 h to remove all water. 1.5 mL of N,N-dimethylformamide (DMF) containing 0.1% trifluoroacetic acid (TFA) was then added to the lyophilized samples and shaken for 6 h, followed by filtration (0.45 μm filters, Whatman, NJ) and analysis of molecular weight using gel permeation chromatography (GPC) using previously described procedures [38], [41]. Molecular weights of degraded samples were compared to that of pristine polymer film.

To evaluate the mass loss from the polymer films, aliquots from degradation media were treated with 1 N NaOH to hydrolyze the terpolymer fragments to DT and PEG, then neutralized by acidification with 12 N HCl followed by high pressure liquid chromatography (HPLC). HPLC analysis gave the amount of DT in the supernatant. The HPLC system consisted of a Waters Alliance 2695 Module, Waters 2487 Dual λ Absorbance Ultraviolet (UV) Detector and Empower Pro Software (Waters Corporation, Milford, MA). The column was a Perkin-Elmer Pecosphere C18 (33 × 4.6 mm; 3 μm particle size; 0258-1064, Waltham, MA). The mobile phase was a mixture of water and methanol containing 0.1% TFA with a gradient of 80:20–40:60 in 6 min. The concentration of DT in the hydrolyzed aliquot was determined from a DT standard calibration curve. The amount of DT that had leached into the

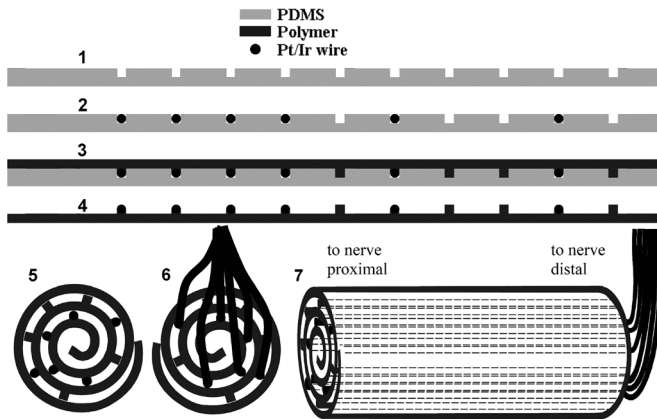


Fig. 2. Fabrication steps of rolled conduit. (1) PDMS mold. (2) placing of wire electrodes. (3) Casting of polymer solution. (4) Formed film with embedded wires. (5) Rolled film, proximal nerve end. (6) Rolled film, distal nerve end. (7) View of constructed conduit; left side attaches to the proximal end of the nerve, right to the distal.

buffer was a good approximation of the extent of erosion of the polymer.

Cast films were tested using a servohydraulic biaxial mechanical testing system coupled with a computerized data acquisition system (MTS, Eden Prairie, MN). Using a 100 Newton load cell, a tensile test was performed uniaxially at a rate of 10 mm/min, five samples per condition in prewarmed media at 37 °C. Degradation samples were removed from incubation media, were measured in the thickness and width dimensions, and placed in the sample holder for testing. Ultimate tensile strength and strain are reported. Thickness measurements were recorded to determine whether swelling occurred during the incubation time in the media.

The effect of particulate leaching and incubation on the morphology of film samples was visualized using scanning electron microscopy (SEM, Amray 1830, Bedford, MA). Incubated film was gently washed with deionized water and lyophilized to remove all water then mounted and sputter-coated with gold palladium (SCD 004 Sputter Coating Unit, Balzers, Liechtenstein) prior to imaging.

C. bRTNi Fabrication and Impedance In Vitro

Teflon coated Pt/Ir microwires 100 μm in diameter (776000, A-M systems, Sequim, WA.) were used as electrodes. Wires were cut to a total length of 150 mm. To provide a recording site, 1–2 mm of wire was exposed at a distance of 1–3 mm from the end of the wire. This allowed for the recording site to be at the inner part of the conduit rather than its face to avoid false recording from nerves that did not regenerate. Indication of regeneration was assumed once recording occurred, since it required growth of tissue into the conduit. Fabrication steps of the bRTNi are as shown in Fig. 2. The description is as follows: 1) a polydimethylsiloxane (Sylgard 184, Fisher Scientific, Pittsburgh, PA) negative mold was fabricated using a custom-made aluminum-machined positive mold with 500 μm grooves with 100 μm depth and 100 μm width; the width of the PDMS mold was trimmed to 5 mm; 2) the distal end of the wires were tightly inserted into the mold grooves and held by the PDMS structure; not all grooves were filled with wires for these preliminary

studies, leaving blank polymer channels that allowed for maintenance of the open architecture of the conduit and generally improving regeneration through a multi-lumen structure [28]; 3) a polymer solution containing porogen was dispensed using a syringe with a 27 g needle on top of the mold (0.3 mL), covering the wires and filling the empty grooves, then dried overnight under a chemical hood; 4) the formed film was adhered to the wires and gently removed from the mold using forceps; 5) the film was rolled to reach 2.5–3.0 mm in diameter, matching the diameter of the sciatic nerve of a rabbit [42]. Excess material was cut and the edge of the film was attached to the main conduit through solvent welding with THF. Illustration of rolled film with embedded wires is seen in Fig. 2 (steps 5 and 6).

To allow additional attachment points and support for the severed nerve ends to the edge of the conduit, two polymer “flaps” were attached via solvent welding to the sides of the conduit. Once all solvent-based procedures were finished, the structure was placed under vacuum at 40 °C for seven days to remove excess THF. The wires protruding from the proximal side of the conduit were bound together above the structure in a manner that allowed spacing between them, reducing (to the extent feasible) the obstruction of the distal end of the conduit by the wires. Wires were placed through a flexible biomedical silicone tubing (807900, A-M systems, Sequim, WA) to bundle and protect them together. This allowed placing the connector subcutaneously for periodical recordings. Connection of the proximal end of the wires was made by soldering 5 mm of exposed wires directly to a 16 channel chronic connector with a protective cap (ZCA-OMN16, Tucker Davis Technologies, Alachua, FL). To avoid infiltration of foreign elements and fluids to the leading wires and tubes, medical grade silicone adhesive was used for sealing (MED ADH 4100 RTV, Bluestar Silicones, East Brunswick, NJ). Removal of glucose from the conduits and generation of porosity was done by sinking tubes in deionized water for 72 h followed by drying under vacuum for one day, then sterilization in ethylene oxide followed by 10–14 days under vacuum at room temperature.

In vitro impedance was measured using a commercial impedance meter designed for microelectrodes (Electrode Impedance Tester, Model 2900, AM-systems, Sequim, WA). Using 2 model bRTNis, each with five embedded electrodes, the distal ends of electrodes were soldered to a pin dip connector (Mill-Max, Oyster Bay, NY) for ease of connection to a measuring device. Measurements were performed by immersing probes in 50 mL of PBS at room temperature using Ag/AgCl reference electrode (BASi, West Lafayette, IN) placed 50 mm from the tested electrode. Impedance was measured with an applied 1000 Hz, 20 nA sine wave immediately after fabrication, particulate leaching, and one week of incubation in PBS at 37 °C.

D. In Vivo Feasibility Study: Implantation, Electrophysiological Recording and Signal Processing

We have evaluated the implantation procedure and signal recording potential of fabricated devices using an experimental protocol approved by the Johns Hopkins Animal Care and Use Committee (ACUC) and the US Army Medical Research and

Material Command Animal Care and Use Review Office. All procedures were compliant with NIH guidelines.

Three New Zealand rabbits, weighing an average of 4.1 kg (3.8–4.4 kg), were anesthetized by administering ketamine (10 mg/kg) and xylazine (5 mg/kg) intravenously, followed by 1.0%–2.0% isoflurane/oxygen applied using a facemask, adjusted to maintain the anesthetized state of the animal throughout the procedure. Strict sterile surgical rules were followed during all experiments. Rabbits were shaved and prepared in the usual fashion. An incision was made along the posterior of the left hind leg at 5 cm and the sciatic nerve was exposed. A tunnel was formed under the skin to allow the covered electronic connector to be placed subcutaneously. The sciatic nerve was cut 1 cm proximal to the bifurcation point of the sciatic nerve in the popliteal fossa. The epineurium of both nerve stumps were sutured first to the device flaps using 9-0 suture under microscope, four times on each side, then directly to the face of the nerve guide conduit. The muscular and skin incisions were closed by layers. The animals had free access to food and water before and after the experiments, and were subjected to a 12 h day/night cycle in a quiet environment.

At predetermined periods, the rabbit was reanesthetized with ketamine and xylazine, shaved and prepared in the usual fashion. At the site of the distal connector touched by the surgeon's finger, a new 0.8 cm incision was made along the skin in the left hind leg. The connector was carefully exposed and interfaced with a Tucker Davis Technologies ZIF16 head-stage connected via a preamplifier. The neuron spike signal in the sciatic nerve from the electrode was recorded continuously for 30 min with 24.14 kHz sampling frequency (RX 5, Tucker-Davis Technologies, Alachua, FL), downsampled to 12 kHz, and fourth-order Butterworth bandpass filtered with forward-backward, zero-phase lag with cutoff frequencies of 700–2000 Hz. A wavelet-based denoising method [43] was used to increase the signal-to-noise ratio. The skin incision was closed by layers. The firing rates of the action potentials were analyzed offline and quantified with MATLAB 7.0.

E. Statistical Methods

Statistical analysis was performed using a computerized statistical package (Statistics Program for the Social Sciences version 16.0, Chicago, IL). Group parametric values were reported as mean \pm SEM and repeated measure of general linear analysis was performed for parametric data with Student's *t*-test for continuous variables.

III. RESULTS

A. Polymer Molecular Weight, Mass Loss, Mechanical Properties and Morphology Changes

All polymers used had starting molecular weight averages of over 150 kD. Fig. 3(A) illustrates the loss in molecular weight (MW) during the first four weeks for series of polymers initially evaluated for use for the bRTNi fabrication. It is clear that all polymers experienced a sharp and immediate loss in MW within the first week, followed by a slower pace of degradation. Polymers which lost more than 50% of their original MW after one week of incubation were omitted from further evaluation.

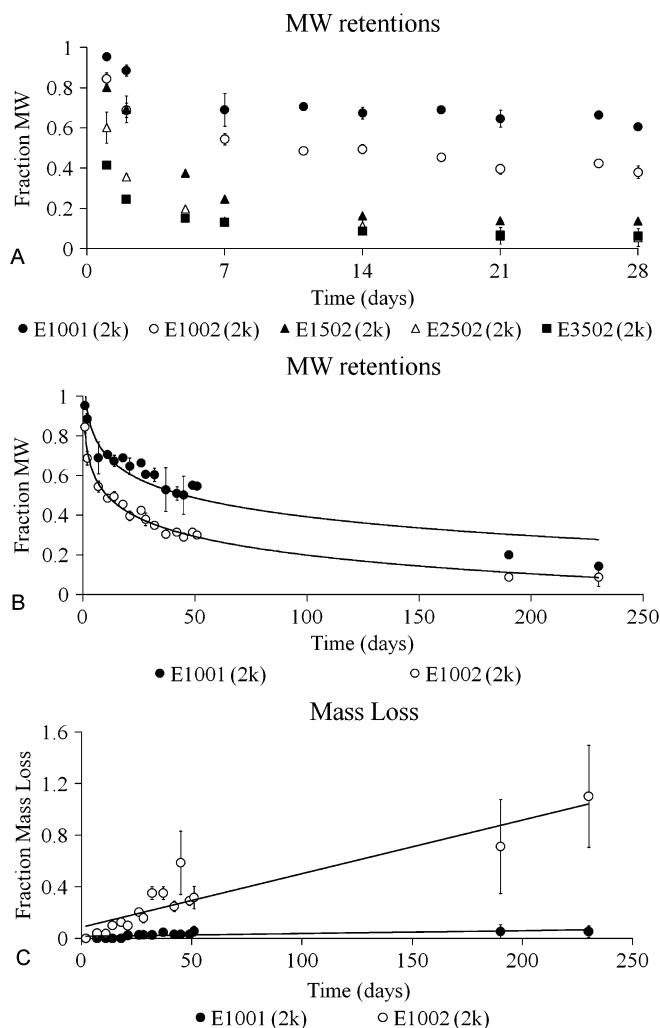


Fig. 3. Fractional molecular weight loss versus time. (A) Four week data collected all polymers. (B) 32 weeks of data collected for promising polymers E1001(2K) and E1002(2K). R^2 values for logarithmic regression are 0.90 and 0.99, respectively. (C) Fraction mass loss and linear regression for E1001(2K) and E1002(2K). R^2 values are 0.85 and 0.47, respectively.

The two promising polymers, E1001(2K) and E1002(2K), were continually evaluated for up to 230 days as shown in Fig. 3(B). By the last time point, the E1002(2K) had completely eroded in the media (see mass loss data) and its molecular weight was reduced by over 90%. The E1001(2K) lost over 85% of its original molecular weight, but did not erode in a significant manner. These findings are confirmed by the mass loss data presented in Fig. 3(C). Clearly the E1001(2K) has minimally eroded. The films were still intact (though fragile to touch). In contrast, the E1002(2K) had completely eroded, and linear regression of the E1002(2K) data reveals total erosion time of 210 days.

Ultimate stress and strain of incubated films are shown in Fig. 4. The mechanical properties test required measurement of dimensions and mounting onto tensile testing clamps, requiring sample mechanical integrity. The zero time point is post glucose leaching. With the faster degrading polymers (those with 15% DT or more), the films collapsed during the second collection. For that reason, only the data for the slower degrading polymers is presented, together with a single example of E1502(2K). The E1001(2K), even though was slower

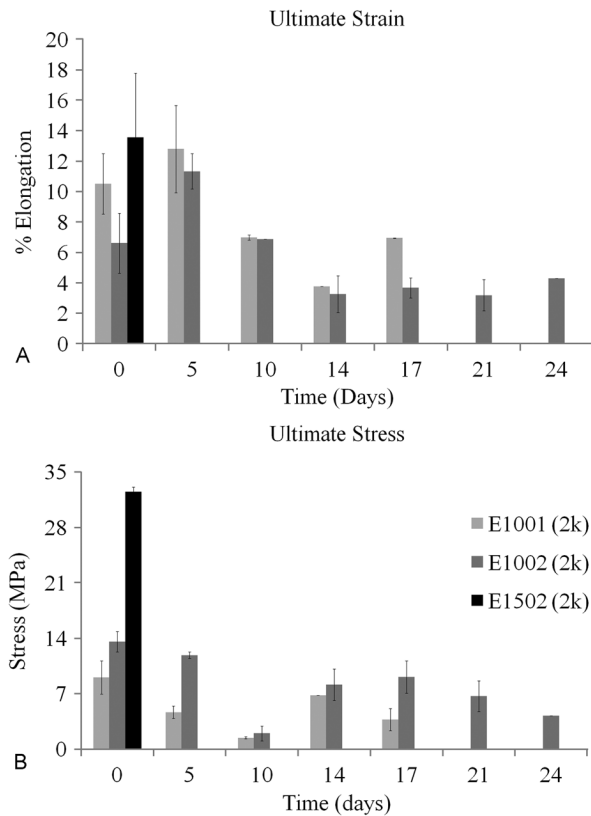


Fig. 4. Over three weeks of ultimate strain (top) and stress (below) results for E1002(2K) compared to E1001(2K) and E1502(2K).

to degrade according to GPC data, was too weak to handle after 17 days. The E1002(2K) kept its integrity for an additional week. The surprising difference in mechanical properties retention could be attributed to the elevated amount of PEG in the E1002(2K). Even through the addition of PEG accelerates the degradation rate of the polymer; it also acts as a plasticizer, increasing the compliance of the polymer and allowing additional time of use. The ultimate stress was usually followed by a reduction in strength until complete failure. While visually inspecting the film during testing, a small tear was initially observed accompanying the reduction in strength, followed by tear propagation and strength reduction till complete failure.

Dimensional retention is presented as a measure of the effect of incubation time on the morphology of degraded films in Fig. 5(A). This data was collected from measurements performed prior to the mechanical testing. Data depicts that the fabrication of the films (prepared at different batches) was consistent, and swelling did not occur (no statistical difference was detected). In the SEM scans in Fig. 5, visual change in porosity is observed after particulate leaching [Fig. 5(B)]. With additional incubation time, connecting fissures between pores are observed, possibly leading to loss of mechanical strength [Fig. 5(C) and (D)].

B. bRTNi Fabrication and Impedance In Vitro

Images of fabricated probes are shown in Fig. 6. In Fig. 6(A), the proximal part of the bRTNi is shown. A structure of 12 channels is visible. 10 channels are formed by active electrode wires

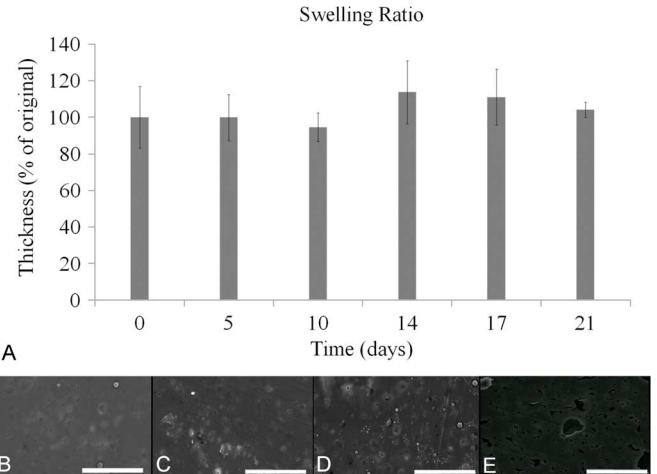


Fig. 5. (A) Dimensional retention (lack of swelling) of E1002(2K) films. Incubated sample thickness was measured against the undegraded samples. (B) SEM images of film samples after particulate leaching, formation of pores is visible (B) after fabrication (C), (D), (E) 10, 21, and 28 days incubation, respectively) connections between pores are formed, materializing as fissures. Scale bar $100\ \mu\text{m}$.

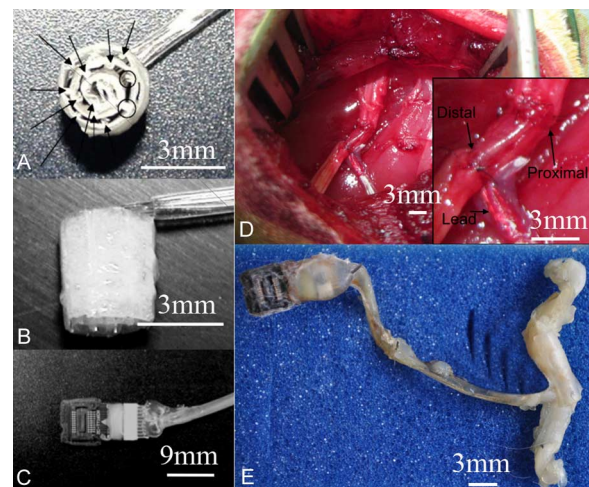


Fig. 6. (A) Cross section view to the proximal part of regenerative electrode tube, arrows mark electrode location, circles mark blank polymer channels. (B) Profile of bRTNi showing lead wires encased in a protective tube. (C) Uncapped ZIF-16 connector. (D) bRTNi with added flaps positioned after implantation. Inserts show distal and proximal end of nerves in respect to the device. (E) Representative specimen of harvested bRTNi after eight weeks.

(marked with arrows). Two are blank polymer (marked with circles). In the background, the lead tube containing the wires is visible. In Fig. 6(B), the same bRTNi is shown from its profile. Fig. 6(C) shows the ZIF connector. Fig. 6(D) illustrates the final structure of the design placed implanted within a rabbit sciatic nerve. Fig. 6(E) illustrates an explanted device after eight weeks. bRTNi is still intact, and nerve shows signs of integration in the device.

Recorded impedance values are presented in Table I. In 2 of the 10 electrodes, the initial impedance was three orders of magnitude higher than in the average of the rest. Once particulate leaching was initiated, all impedance values dropped to a similar range. It is possible that during the fabrication, a thin layer of polymer solution surrounded some of the electrodes. As the

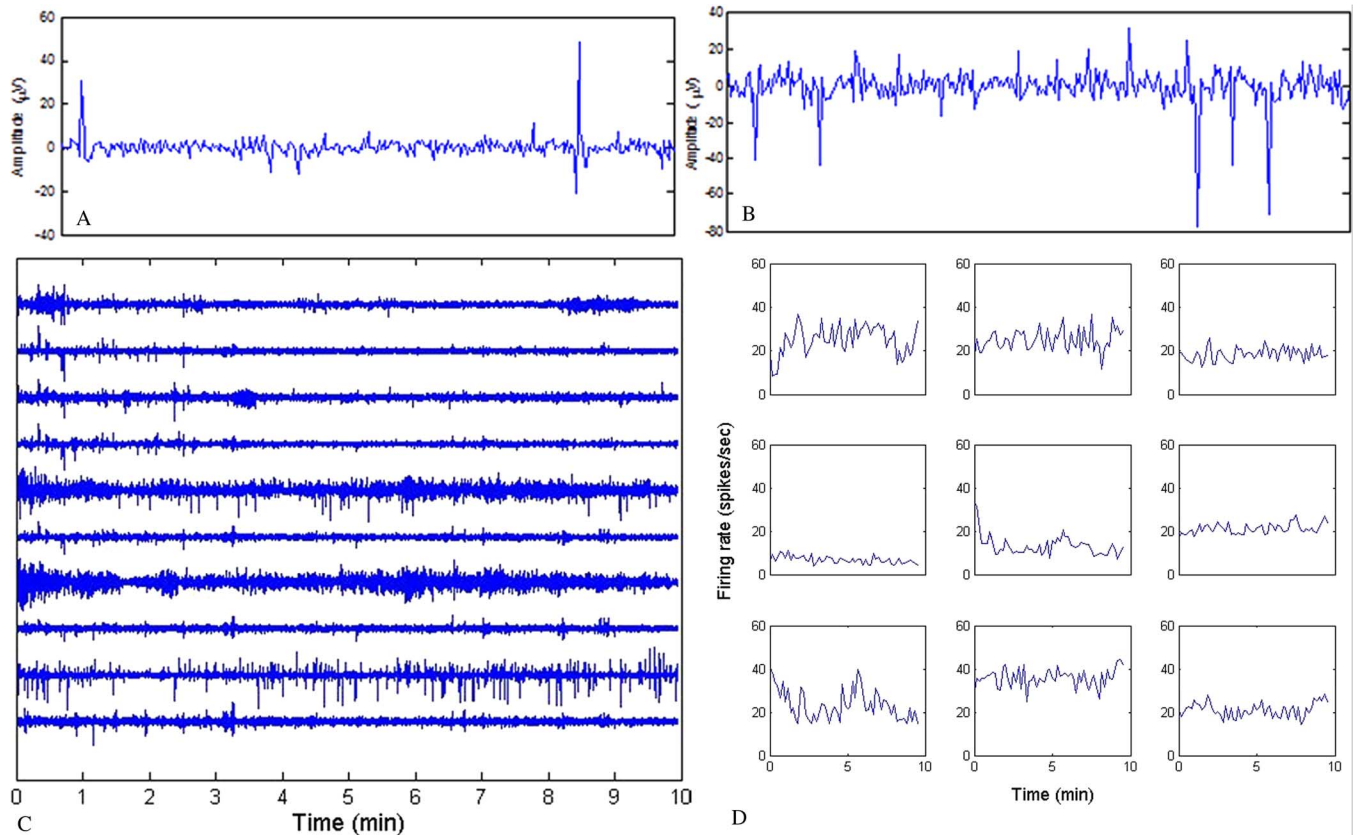


Fig. 7. (A) Representative 10 s plot of single channel four weeks postimplantation. (B) Representative 10 s plot of single channel eight weeks postimplantation. (C) Representative plots of multichannels of peripheral nerve spiking activities eight weeks postimplantation. (D) Firing rates of multichannels eight weeks postimplantation.

TABLE I
BRTNi IMPEDANCE CHANGE AFTER PARTICULATE LEACHING

Electrode #	Impedance (kOhm)	Impedance (kOhm)	Impedance (kOhm)
	0 days immersion	1 day immersion	7 days immersion
1	71	10	9
2	1500	12	6
3	48	2	2
4	5	2	2
5	3	3	1
6	5	2	2
7	3	1	2
8	2	3	2
9	1600	6	3
10	5	1	2

polymer is a dielectric material, it may have caused the formation of an insulating layer around the recording site. Once the polymer is exposed to the aqueous environment, this thin layer is removed (via degradation/erosion), allowing the exposure of the recording site and reduction in impedance values.

C. In Vivo Electrophysiological Feasibility Study

Representative neuronal spikes are shown in Fig. 7. Neural spike signals with signal-to-noise ratios (SNR) ≥ 2.0 , and peak-to-peak amplitudes from 40–120 μV were successfully recorded for at least eight weeks following chronic implanta-

tion. At two weeks after implantation, no obvious neural spike signal was detected. Signals started to appear at four weeks postimplantation [Fig. 7(A)], and became stronger at eight weeks postimplantation [Fig. 7(B)–(D)]. The average firing rate of the multichannel recorded signals was higher at eight weeks postimplantation (21.7 ± 2.2 spikes/s) than four weeks postimplantation (12.9 ± 1.9 spikes/s) ($p = 0.006$).

IV. DISCUSSION

Our study demonstrates that a biodegradable terpolymer is able to be tuned to degrade at a rate that is slow enough to possibly match neural regeneration, yet fast enough to allow nerve freedom once regeneration is complete. Our polymer system is based on novel variation of the tyrosine-derived polycarbonate terpolymers. These are known to be biocompatible [36], [44], [45] and their tunable properties are primarily influenced by polymer composition [36], [38], [46], [47]. Unlike conventional biodegradable polymers, they do not form acidic environments as they degrade, preventing localized toxicity [36], [48]. The addition of PEG blocks modulated water absorption of the polymer due to their intrinsic hydrophilic properties [47], which in turn modulated degradation rate and mechanical properties (enhanced flexibility). The addition of DT monomer increases the initial rigidity of the polymer, yet also significantly increases the degradation rate of the polymer. The DTE block allows for stability and strength. Fine tuning of the three monomer compositions is required to achieve optimization of degradation rate and structural properties for a specific

applications. A wide variety of polymers and designs have been applied for degradable conduits. From simple hollow tubes [33] to multiluminal or grooved tubes [49], and fiber-filled tubes [50], [51], where the lumens and fibers act as guiding objects for axonal regrowth. Interestingly, the degradation rates of the polymers have not been reported. In one particular study, where the degradation rate of collagen tubes was associated with the quality of critical gap regeneration, a 2–3 week half life for implants was found to be ideal. Our chosen polymer, E1002(2K), was found *in vitro* to lose 50% of its molecular weight within two weeks, maintain its mechanical integrity for over three weeks, and completely erode within 25 weeks. Feng *et al.* suggest preferred degradation of the polymer within 12 weeks [31]. Consistent with other studies [52], [53], our degradation/erosion evaluations were performed *in vitro*. In the case of mass loss, *in vivo* reduction in polymer mass may be accelerated due to greater mass transport and the presence of solubilizing factors [54].

Among the many technologies explored for direct neuronal interfacing, the regenerative device could have great benefits due to its exploitation of the regenerative property of amputated peripheral nerves. This can occur even without the presence of a distal stump and specifically by the assistance of muscular reinnervation [30], [55], [56]. The use of longitudinal regenerative channels with recording ability has been of high interest and could result in high fidelity recording; a few designs of this nature have been suggested [19], [25], yet with none of them is the conduit is fully degradable. We have used Pt/Ir based wires for their availability, simplicity of use, and proven record as functional intrafascicular electrodes [32]. Our fabrication technique allows for future adoption of use of polyLIFE [57] as the recording moiety (replacing the Pt/Ir wires in the conduit). Replacing the current Pt/Ir wires with polyLIFE could provide: 1) an increase in the mechanical match between nerves and electrodes remaining after conduit resorption, 2) an increase in the number of electrodes available for recording in the conduit due to their smaller size, and 3) minimized obstruction of the distal end of the conduit by the lead wires to the connector. This will result in a fully degradable conduit with remaining free electrodes, and could be made possible through minor modifications such as change in groove depth and spacing in the PDMS mold design.

An ideal regenerative scaffold should obtain mechanical properties that are at the same order of magnitude of those of the inherent tissue, allowing healthy regeneration through initial protection of the growing organ. Avoidance of stress shielding at the latter stages of regeneration is also required. In environments where external forces may be applied on the implantation site, failure of the device itself (an “adhesive” failure) is preferred over the failure of the regenerating tissue (a “cohesive” failure). This minimizes the potential of inflicting additional damage on the regenerating tissue. The strength of a regenerative device should reduce with time in accordance to the tissue becoming healthier and stronger. These were guidelines used in the selection criteria for the polymer. Healthy peripheral nerves under tension exhibit an initial toe region for the first 5%–15% of strain [58] and a 12 MPa [59] ultimate strength. We identified that the E1002(2K) maintained strength

that is just under that of a nerve for over three weeks (12 to 4 MPa in 24 days). The E1002(2K) strain fits within the range of the toe region of a nerve (12% to 4%), thus avoiding a mechanical properties mismatch. Reports that severed nerves retain over 50% of their recovered tensile strength within 1–4 weeks of repair (i.e., approximately 6 MPa) [60] allow us to assume that our polymer is suitable for use as a regenerative construct for injured nerves.

Measurements of sample dimensions prior to mechanical testing revealed little swelling of the E1001(2K) and E1002(2K) during the incubation period. The lack of swelling indicates dimensional stability that is essential for nerve guide conduits, as polymer swelling could lead to steric obstruction of nerve growth and even nerve compression [61].

We have been able to use simple a polymer fabrication technique to demonstrate the potential in fabricating a high electrode count biodegradable conduit. *In vitro* impedance data revealed recording potential that is maintained over time. Action potentials from severed sciatic nerves were successfully recorded in real time. We have combined best-of-breed concepts from existing regeneration-type sieve electrodes, nerve guidance channels and biodegradable polymers. In this work, we did not address the long term biocompatibility effect of the implantation on the physiological health of the tissue. However, this study was intended as a proof of design with a limited *in vivo* characterization. Our main goal was to develop a biodegradable regenerative-type neural interface and successfully demonstrate the recording potential of our design, which were both achieved. Future work will allow our design to further serve its multiple function potential by: 1) providing a microstructured mechanical scaffold for regenerating fibers, 2) promoting neurite ingrowth through the application of electric fields, 3) applying chemical mediators to allow for unrestricted axonal growth, and 4) positioning active electrode sites within closer proximity of nerve fibers. In addition, successful development of this technology will have implications for nerve repair in clinical settings, as variations of the proposed devices could be used in place of autologous nerve grafts. Future long-term and larger *in vivo* studies, including quantitative biocompatibility research are needed to verify the long-term *in vivo* effect.

V. CONCLUSION

This study has shown that our biodegradable polymer created via our unique fabrication technique obtains the mechanical and degradation retention properties required from nerve regeneration apparatus. An eight-week successful recording session has demonstrated that our biodegradable regenerative type neural interface is a good candidate for chronic high fidelity recording electrodes for integration in the regeneration of peripheral nerves. This study also provides additional new control sources for the future development of new nerve signal controlled prosthetics.

ACKNOWLEDGMENT

The authors would like to thank Dr. R. Rojas for his help in the polymers synthesis within this study and M. Fifer for his editorial support.

REFERENCES

- [1] K. Ziegler-Graham *et al.*, "Estimating the prevalence of limb loss in the United States: 2005 to 2050," *Arch. Phys. Med. Rehabil.*, vol. 89, pp. 422–429, Mar. 2008.
- [2] D. Datta and V. Ibbotson, "Prosthetic rehabilitation of upper limb amputees: A five year review," *Clin Rehabil.*, vol. 5, pp. 311–316, 1991.
- [3] X. Jia *et al.*, "Residual motor signal in long-term human severed peripheral nerves and feasibility of neural signal-controlled artificial limb," *J. Hand Surg. Am.*, vol. 32, pp. 657–666, May–Jun. 2007.
- [4] G. S. Dhillon and K. W. Horch, "Direct neural sensory feedback and control of a prosthetic arm," *IEEE Trans. Neural Syst. Rehabil. Eng.*, vol. 13, no. 4, pp. 468–472, Dec. 2005.
- [5] G. S. Dhillon *et al.*, "Residual function in peripheral nerve stumps of amputees: Implications for neural control of artificial limbs," *J. Hand Surg. Am.*, vol. 29A, pp. 605–615, Jul. 2004.
- [6] X. Jia *et al.*, "The original report of the first experimental study on electric prosthesis controlled by signals of nerves in amputation stump of human," *Chin. J. Phys. Med. Rehabil.*, vol. 26, pp. 20–23, 2004.
- [7] R. R. Harrison *et al.*, "Wireless neural recording with single low-power integrated circuit," *IEEE Trans. Neural Syst. Rehabil. Eng.*, vol. 17, no. 4, pp. 322–329, Aug. 2009.
- [8] P. J. Rousche and R. A. Normann, "Chronic recording capability of the Utah intracortical electrode array in cat sensory cortex," *J. Neurosci. Methods*, vol. 82, pp. 1–15, Jul. 1, 1998.
- [9] F. V. Tenore *et al.*, "Decoding of individuated finger movements using surface electromyography," *IEEE Trans. Biomed. Eng.*, vol. 56, no. 5, pp. 1427–1434, May 2009.
- [10] N. Jiang *et al.*, "Extracting simultaneous and proportional neural control information for multiple-DOF prostheses from the surface electromyographic signal," *IEEE Trans. Biomed. Eng.*, vol. 56, no. 4, pp. 1070–1080, Apr. 2009.
- [11] T. A. Kuiken *et al.*, "Targeted reinnervation for enhanced prosthetic arm function in a woman with a proximal amputation: A case study," *Lancet*, vol. 369, pp. 371–380, 2007.
- [12] X. Navarro *et al.*, "A critical review of interfaces with the peripheral nervous system for the control of neuroprostheses and hybrid bionic systems," *J. Peripher. Nerv. Syst.*, vol. 10, pp. 229–258, Sep. 2005.
- [13] P. N. Sergi *et al.*, "Biomechanical characterization of needle piercing into peripheral nervous tissue," *IEEE Trans. Biomed. Eng.*, vol. 53, no. 11, pp. 2373–2386, Nov. 2006.
- [14] M. Gasson *et al.*, "Invasive neural prosthesis for neural signal detection and nerve stimulation," *Int. J. Adaptive Control Signal Process.*, vol. 19, pp. 365–375, Jun. 2005.
- [15] K. Warwick *et al.*, "The application of implant technology for cybernetic systems," *Arch. Neurol.*, vol. 60, pp. 1369–1373, Oct. 1, 2003, 2003.
- [16] A. Mannard *et al.*, "Regeneration electrode units: Implants for recording from single peripheral nerve fibers in freely moving animals," *Science*, vol. 183, pp. 547–549, Feb. 8, 1974.
- [17] F. Castro *et al.*, "Fiber composition of the rat sciatic nerve and its modification during regeneration through a sieve electrode," *Brain Res.*, vol. 1190, pp. 65–77, Jan. 2008.
- [18] S. P. Lacour *et al.*, "Polyimide micro-channel arrays for peripheral nerve regenerative implants," *Sensors Actuators a-Physical*, vol. 147, pp. 456–463, Oct. 2008.
- [19] T. Suzuki *et al.*, "Bundled microfluidic channels for nerve regeneration electrodes," in *Proc. 3rd Int. IEEE/EMBS Conf. Neural Eng.*, 2007, pp. 17–18.
- [20] J. J. FitzGerald *et al.*, "Microchannel electrodes for recording and stimulation: In vitro evaluation," *IEEE Trans. Biomed. Eng.*, vol. 56, no. 5, pp. 1524–1534, May 2009.
- [21] G. T. A. Kovacs *et al.*, "Silicon-substrate microelectrode arrays for parallel recording of neural activity in peripheral and cranial nerves," *IEEE Trans. Biomed. Eng.*, vol. 41, no. 6, pp. 567–577, Jun. 1994.
- [22] X. Navarro *et al.*, "Peripheral nerve regeneration through microelectrode arrays based on silicon technology," *Restorative Neurol. Neurosci.*, vol. 9, pp. 151–160, Apr. 1996.
- [23] D. Ceballos *et al.*, "Morphologic and functional evaluation of peripheral nerve fibers regenerated through polyimide sieve electrodes over long-term implantation," *J. Biomed. Mater. Res.*, vol. 60, pp. 517–528, Jun. 2002.
- [24] P. Negrodo *et al.*, "Differential growth of axons from sensory and motor neurons through a regenerative electrode: A stereological, retrograde tracer, and functional study in the rat," *Neuroscience*, vol. 128, pp. 605–6015, 2004.
- [25] S. H. Cho *et al.*, "Biocompatible SU-8-based microprobes for recording neural spike signals from regenerated peripheral nerve fibers," *IEEE Sensors J.*, vol. 8, no. 11, pp. 1830–1836, Nov. 2008.
- [26] T. A. Hadlock *et al.*, "A new artificial nerve graft containing rolled Schwann cell monolayers," *Microsurgery*, vol. 21, pp. 96–101, 2001.
- [27] C. Sundback, A. Huang, T. Sheahan, M. Lawlor, J. Vacanti, and T. Hadlock, "Peripheral nerve regeneration guided by multi-channeled rolled conduits [Abstract]," in *Proc. 2006 World Congress Tissue Eng. Regenerative Med.*, 2006.
- [28] G. C. W. Ruiters *et al.*, "Designing ideal conduits for peripheral nerve repair," *Neurosurg. Focus*, vol. 26, Feb. 2009.
- [29] T. Hadlock *et al.*, "A tissue-engineered conduit for peripheral nerve repair," *Arch. Otolaryngol. Head Neck Surg.*, vol. 124, pp. 1081–1086, Oct. 1, 1998.
- [30] S. Micera *et al.*, "On the use of longitudinal intrafascicular peripheral interfaces for the control of cybernetic hand prostheses in amputees," *IEEE Trans. Neural Syst. Rehabil. Eng.*, vol. 16, no. 5, pp. 453–472, Oct. 2008.
- [31] X. Feng *et al.*, "In vitro and in vivo evaluation of a biodegradable chitosan-PLA composite peripheral nerve guide conduit material," *Microsurgery*, vol. 28, pp. 471–479, 2008.
- [32] X. Jia *et al.*, "Improved long-term recording of nerve signal by modified intrafascicular electrodes in rabbits," *Microsurgery*, vol. 28, pp. 173–178, 2008.
- [33] F. Xie *et al.*, "In vitro and in vivo evaluation of a biodegradable chitosan-PLA composite peripheral nerve guide conduit material," *Microsurgery*, vol. 28, pp. 471–479, 2008.
- [34] J. Kohn and R. Langer, "Polymerization reactions involving the side-chains of alpha-L-amino acids," *J. Am. Chem. Soc.*, vol. 109, pp. 817–820, Feb. 1987.
- [35] A. J. Asikainen *et al.*, "Tyrosine-derived polycarbonate membrane in treating mandibular bone defects. An experimental study," *J. R. Soc. Interface*, vol. 3, pp. 629–635, Oct. 2006.
- [36] S. L. Bourke and J. Kohn, "Polymers derived from the amino acid L-tyrosine: Polycarbonates, polyarylates and copolymers with poly(ethylene glycol)," *Adv. Drug Delivery Rev.*, vol. 55, pp. 447–466, Apr. 2003.
- [37] S. D. Abramson, "Selected bulk and surface properties and biocompatibility of a new class of Tyrosine-derived polycarbonates," Ph.D. dissertation, Dept. Biomed. Eng., Rutgers Univ., 2002.
- [38] J. Schut *et al.*, "Glass transition temperature prediction of polymers through the mass-per-flexible-bond principle," *Polymer*, vol. 48, pp. 6115–6124, 2007.
- [39] B. A. Harley *et al.*, "Optimal degradation rate for collagen chambers used for regeneration of peripheral nerves over long gaps," *Cells Tissues Organs*, vol. 176, pp. 153–165, 2004.
- [40] M. S. K. Recknor J.B., "Nerve regeneration: Tissue engineering strategies," in *The Biomedical Engineering Handbook: Tissue Engineering and Artificial Organs*, J. D. Bronzino, Ed., 3rd ed. Boca Raton: CRC, 2006, p. 1304.
- [41] R. Rojas *et al.*, "Evaluation of automated synthesis for chain and step-growth polymerizations: Can robots replace the chemists?," *J. Polymer Sci. Part a-Polymer Chem.*, vol. 47, pp. 49–58, Jan. 2009.
- [42] S. Jun *et al.*, "Magnetic resonance microneurography of rabbit sciatic nerve on a 1.5-T clinical MR system correlated with gross anatomy," *Microsurgery*, vol. 28, pp. 32–36, 2008.
- [43] A. Diedrich *et al.*, "Analysis of raw microneurographic recordings based on wavelet de-noising technique and classification algorithm: Wavelet analysis in microneurography," *IEEE Trans. Biomed. Eng.*, vol. 50, no. 1, pp. 41–50, Jan. 2003.
- [44] V. Tangpasuthadol *et al.*, "Hydrolytic degradation of tyrosine-derived polycarbonates, a class of new biomaterials. Part I: Study of model compounds," *Biomaterials*, vol. 21, pp. 2371–2378, Dec. 2000.
- [45] K. A. Hooper *et al.*, "Comparative histological evaluation of new tyrosine-derived polymers and poly(L-lactic acid) as a function of polymer degradation," *J. Biomed. Materials Res.*, vol. 41, pp. 443–454, Sep. 1998.
- [46] C. Yu and J. Kohn, "Tyrosine-PEG-derived poly(ether carbonate)s as new biomaterials—Part I: Synthesis and evaluation," *Biomaterials*, vol. 20, pp. 253–264, Feb. 1999.
- [47] A. Sousa *et al.*, "Nanoscale morphological changes during hydrolytic degradation and erosion of a bioresorbable polymer," *Macromolecules*, vol. 39, pp. 7306–7312, 2006.
- [48] B. Schlosshauer *et al.*, "Synthetic nerve guide implants in humans: A comprehensive survey," *Neurosurgery*, vol. 59, pp. 740–747, Oct. 2006.
- [49] C. Sundback *et al.*, "Manufacture of porous polymer nerve conduits by a novel low-pressure injection molding process," *Biomaterials*, vol. 24, pp. 819–830, Feb. 2003.

- [50] K. Matsumoto *et al.*, "Peripheral nerve regeneration across an 80-mm gap bridged by a polyglycolic acid (PGA)-collagen tube filled with laminin-coated collagen fibers: A histological and electrophysiological evaluation of regenerated nerves," *Brain Res.*, vol. 868, pp. 315–328, Jun. 2000.
- [51] W. M. Fan *et al.*, "Repairing a 35-mm-long median nerve defect with a chitosan/PGA artificial nerve graft in the human: A case study," *Microsurgery*, vol. 28, pp. 238–242, 2008.
- [52] I. Pomerantseva *et al.*, "Degradation behavior of poly(glycerol sebacate)," *J. Biomed. Materials Res. Part A*, vol. 91A, pp. 1038–1047, Dec. 2009.
- [53] B. G. Amsden *et al.*, "In vivo degradation behavior of photocross-linked star-poly(μ -caprolactone-co-d,l-lactide) Elastomers," *Biomacromolecules*, vol. 7, pp. 365–372, 2005.
- [54] M. V. Chaubal *et al.*, "In vitro and in vivo degradation studies of a novel linear copolymer of lactide and ethylphosphate," *J. Biomater. Sci.-Polymer*, vol. 14, pp. 45–61, 2003.
- [55] T. A. Kuiken *et al.*, "Redirection of cutaneous sensation from the hand to the chest skin of human amputees with targeted reinnervation," in *Proc. Nat. Acad. Sci. USA*, 2007, vol. 104, pp. 20061–20066.
- [56] N. Lago and X. Navarro, "Evaluation of the long-term regenerative potential in an experimental nerve amputee model," *J. Peripheral Nervous Syst.*, vol. 12, pp. 108–120, Jun. 2007.
- [57] S. M. Lawrence *et al.*, "Fabrication and characteristics of an implantable, polymer-based, intrafascicular electrode," *J. Neurosci. Methods*, vol. 131, pp. 9–26, 2003.
- [58] K. S. Topp and B. S. Boyd, "Structure and biomechanics of peripheral nerves: Nerve responses to physical stresses and implications for physical therapist practice," *Phys. Therapy*, vol. 86, pp. 92–109, Jan. 2006.
- [59] M. K. Kwan *et al.*, "Strain, stress and stretch of peripheral nerve rabbit experiments in vitro and in vivo," *Acta Orthopaedica*, vol. 63, pp. 267–272, 1992.
- [60] C. L. F. Temple *et al.*, "Tensile strength of healing peripheral nerves," *J. Reconstructive Microsurg.*, vol. 19, pp. 483–488, Oct. 2003.
- [61] V. Mukhatyar *et al.*, "Tissue engineering strategies designed to realize the endogenous regenerative potential of peripheral nerves," *Adv. Materials*, vol. 21, pp. 4670–4679, Dec. 2009.



Dan Lewitus received the B.S. degree in plastics engineering from the Shenkar College of Engineering and Design, Israel, in 2000, and the M.S. degree in plastics engineering from the University of Massachusetts, Lowell, in 2004. He is currently working toward the Ph.D. degree in biomedical engineering at the New Jersey Center for Biomaterials, Rutgers University, New Brunswick, NJ.

His research involves developing biodegradable polymer systems for neural prosthetics both in the central and peripheral nervous systems. In between

his degrees and prior to his Ph.D. studies, he worked both in Israel and Germany on developing of performance enhancing additives for the polymer processing industry.



R. Jacob Vogelstein received the Sc.B. degree in neuroengineering from Brown University, Providence, RI, and the Ph.D. degree in biomedical engineering from the Johns Hopkins University School of Medicine, Baltimore, MD.

He is the Assistant Program Manager for Applied Neuroscience at the Johns Hopkins University (JHU) Applied Physics Laboratory and an Assistant Research Professor in Electrical Engineering at the JHU's Whiting School. He has worked on neuroscience technology for over a decade, focusing

primarily on neuromorphic systems and closed-loop brain-machine interfaces. His research has been featured in a number of prominent scientific and engineering journals including the IEEE TRANSACTIONS ON NEURAL SYSTEMS AND REHABILITATION ENGINEERING, the IEEE Transactions on Biomedical Circuits and Systems, and the IEEE TRANSACTIONS ON NEURAL NETWORKS.



Gehua Zhen received the M.D. degree in clinical medicine from Shanghai Medical University, Shanghai, China, in 1997. She completed her surgery residency and fellowship and was an attending surgeon in the Shanghai 6th People's Hospital, Shanghai. She was a postdoctoral fellow in Johns Hopkins University School of Medicine from 2005 to 2010.

She has been a Faculty in the Department of Orthopedic Surgery, Johns Hopkins University School of Medicine, Baltimore, MD, since 2010.



Young-Seok Choi (M'07) received the B.S. degree in electronic and electrical engineering from Hanyang University, Seoul, Korea, in 2000, and the Ph.D. degree in electrical and computer engineering from Pohang University of Science and Technology (POSTECH), Pohang, Korea, in 2007. From 2007 to 2010, he was a Postdoctoral Fellow in the Department of Biomedical Engineering, Johns Hopkins University School of Medicine, Baltimore, MD.

Since July 2010, he is with the Neural Interface Research Team, Electronics and Telecommunications Research Institute, Daejeon, Korea, where he is currently a Senior Researcher. His current research interests include neural signal processing, brain-computer interface, neural interface, and neural engineering.

Joachim Kohn is a Board of Governors Professor of Chemistry at Rutgers University. He has served as Director of the New Jersey Center for Biomaterials since its establishment in 1997. He is a Fellow of the American Institute for Medical and Biological Engineering (AIMBE) and the Chair of the International College of Fellows of Biomaterials Science and Engineering. He is the principal investigator of several leading federally-funded R&D programs: NIH-funded postdoctoral training program in Tissue Engineering, NIH funded National Resource for Polymeric Biomaterials (RESBIO), the DoD-funded Center for Military Biomaterials Research (CeMBR) and the DoD-funded Armed Forces Institute for Regenerative Medicine (AFIRM). His research interests focus on the development of new biomaterials. He pioneered the use of combinatorial and computational methods for the optimization of biomaterials for specific medical applications. He is mostly known for his seminal work on "pseudo-poly(amino acid)s". He has published over 200 scientific manuscripts and reviews, and holds 45 patents.

Stuart Harshbarger, photograph and biography not available at the time of publication.



Xiaofeng Jia received the M. D. degree in clinical medicine from Zhejiang Medical University, Zhejiang, China, in 1994, the M.S. degree in surgery from Shanghai Medical University, Shanghai, China, in 1997, and the Ph.D. degree in surgery (orthopedics) from Fudan University, Shanghai, China, in 2003.

He has been a Faculty in the Department of Biomedical Engineering, Physical Medicine and Rehabilitation, Johns Hopkins University School of Medicine, Baltimore, MD, since 2007. He completed

his surgery residency in the Huashan Hospital and Orthopedic Surgery fellowship in the Shanghai 6th People's Hospital, Shanghai, China. Later, he was an Attending Orthopedic Surgeon in Shanghai 6th People's Hospital and Zhongshan Hospital, Shanghai. His current research interests include novel application of neuro-electrophysiology for detection and restoration of peripheral nerve and spinal cord injury, therapeutic hypothermia of brain and spinal cord after global ischemia injury.

Dr. Jia is a member of the American Academy of Orthopaedic Surgeons, American Association for Hand Surgery, Society of Critical Care Medicine, American Heart Association. He is a recipient of the 2008 Annual Research Awards from American Association for Hand Surgery, the 2009 Top 20 Scientific Exhibits and the 2008 Finalist of Best Overall Poster Award of American Academy of Orthopaedic Surgeons, the 2007 Cardiopulmonary, Perioperative and Critical Care Junior Investigator Travel Award from American Heart Association, the 2008 Finalist of Research Citation Award from Society of Critical Care Medicine.